Utilizing supercomputing to analyze risks of an emergent large-scale debris field in low earth orbit*

David Buehler

Air Force Institute of Technology, Wright-Patterson AFB, Ohio

Dane Fuller

Air Force Institute of Technology, Wright-Patterson AFB, Ohio

John Colombi

Air Force Institute of Technology, Wright-Patterson AFB, Ohio

William Wiesel

Air Force Institute of Technology, Wright-Patterson AFB, Ohio

Dave Meyer

Air Force Institute of Technology, Wright-Patterson AFB, Ohio

Richard Cobb

Air Force Institute of Technology, Wright-Patterson AFB, Ohio

ABSTRACT

The likelihood of on-orbit breakups, whether spontaneous or the result of collision, will likely continue to grow as the barriers of entry to and use of space are reduced. In all orbital regimes, especially Low Earth Orbit (LEO), preparation to respond quickly when the next breakup occurs is critical. This research utilizes high-performance parallel computation along with Python-driven Systems Tool Kit (STK) to model a large-scale on-orbit breakup in LEO, with the goal to meet a proposed operational need of notification within 90 minutes. The simulated breakup is characterized by the National Aeronautics and Space Administration (NASA) EVOLVE 4.0 breakup model and is completely scalable. The debris field is analyzed over the course of one week using Gabbard plots. The risk posed by the breakup is determined using STK's Advanced Close Approach Tool (ACAT) to report minimum range, minimum separation, and likelihood of collision between the debris and catalog objects. The field is screened for close approaches each day of the week and the probability of collision is computed using multiple linear conjunction models (Alfano, Patera, Chan, & Alfano Maximum Likelihood) to observe how different models predict the likelihood of collision. This research represents the first steps toward being prepared to respond in the event of an on-orbit breakup.

*The views expressed in this paper are those of the authors and do not reflect the official policy or position of the United States Air Force, the Department of Defense, or the U.S. Government.

1 INTRODUCTION

Space debris has been defined by the United Nations Office for Outer Space Affairs as, "Any manmade object in earth orbit or reentering the atmosphere that is nonfunctional [1]." It is currently estimated that there are several million pieces of space debris in orbit around Earth. This debris comes in all shapes and sizes, from one-millimeter flecks of paint to large "dead" satellite bodies weighing nearly 9 tons [2]. While the existing debris poses a serious and persistent threat to all assets in space, the most dangerous pieces are those that have not yet formed. That is, debris that is the result of a sudden unexpected collision or explosion in space. Currently, 10 cm and larger objects in space are reliably tracked. Below 10 cm it is assumed that the objects do not have enough mass to initiate a Kessler syndrome where debris cascades and would ultimately render LEO a graveyard. Small objects on this scale, while not typically large enough to cause significant fragmentation, have been known to cause deteriorative damage to solar panels [3].

The current collision avoidance schema involves the generation of Joint Space Operations Center (JSpOC) collision warnings between known, cataloged objects several days in advance of the conjunction. When a sudden, unexpected breakup occurs, this concept will not provide a timely warning to operators with assets in or near the affected orbit. Historical data shows that it can be reasonably expected to take about two weeks to track down the bulk of the pieces from an on-orbit breakup in LEO [4]. In this two-week absence of actual observations, modeling and simulation can fill the knowledge gap to help guide satellite operators something. This gives operators an idea of what they might expect to encounter, allowing for an informed "maneuver or hold" decision to be made.

1.1 Background

As of 30 May 2018, there are currently 19,122 objects in the public catalog of on-orbit objects, of which 14,331 (~75%) are debris. In January 2007, the worst breakup today occurred as a result of an antisatellite (ASAT) test conducted by China on their own Fengyun-1C (FY-1C) spacecraft. The explosion occurred at 865 kilometers and resulted in 3,400 trackable objects being added to the catalog. Just two years later, Iridium 33 and Cosmos 2251 collided at an altitude just under 800 kilometers, generating more than 2,200 trackable pieces of debris. These two events alone increased the catalog size by 65%. The two events can be clearly seen in Figure 1 [5], [6].

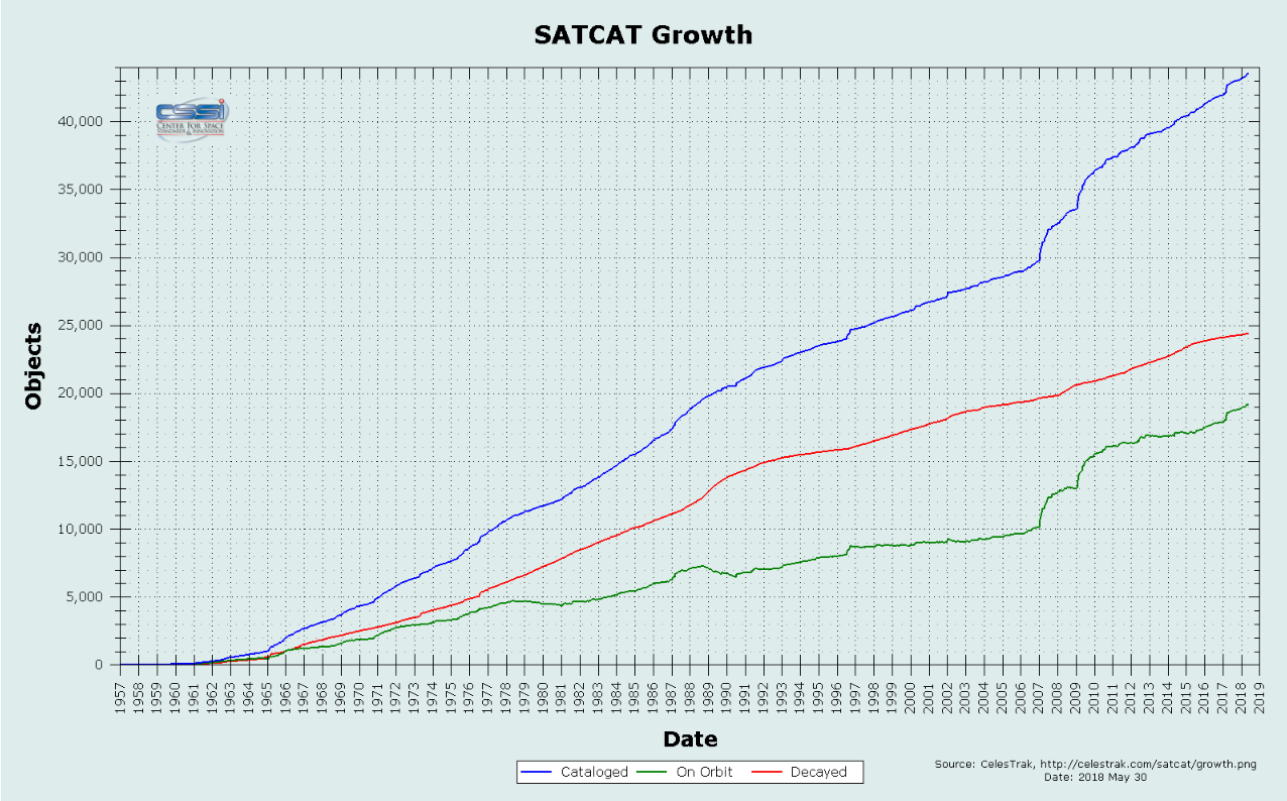

Figure 1. Public satellite catalog as of the end of May 2018.

Other than the two noted events above, debris can come from a number of sources. It can come from scientific experiments like Westford needles, micro-meteorite strikes, or collisions with other pieces of debris. Most commonly however, it comes from exploding defunct rocket bodies. Table 1 was compiled by NASA and shows the top ten breakups as of May 2010, where more than half of these breakups were caused by rocket bodies [7].

Table 1. Top ten breakups as of May 2010.

Common Name	Year of Breakup	Altitude of Breakup	Cataloged Debris*	Debris in Orbit*	Cause of Breakup
Fengyun-1C	2007	850 km	2841	2756	Intentional Collision
Cosmos 2251	2009	790 km	1267	1215	Accidental Collision
STEP 2 Rocket Body	1996	625 km	713	63	Accidental Explosion
Iridium 33	2009	790 km	521	498	Accidental Collision
Cosmos 2421	2008	410 km	509	18	Unknown
SPOT 1 Rocket Body	1986	805 km	492	33	Accidental Explosion
OV 2-1 / LCS 2 Rocket Body	1965	740 km	473	36	Accidental Explosion
Nimbus 4 Rocket Body	1970	1075 km	374	248	Accidental Explosion
TES Rocket Body	2001	670 km	370	116	Accidental Explosion
CBERS 1 Rocket Body	2000	740 km	343	189	Accidental Explosion
			Total: 7903	Total: 5172	

* As of May 2010

When these breakup events occur, the general growth of the debris field over time is well-understood. Initially, the debris will expand into a spherical cloud, like one would expect of an explosion. Very soon after the initial expansion, the orbits of the debris pieces will form a localized "belt" of sorts. Since all of this debris came into existence roughly the same point in orbit, all pieces will share the breakup point as part of their individual orbits. This breakup point is known as the pinch point and is where the greatest density of objects will pass through. As time goes on, the Earth's oblateness will cause nodal precession as defined by Equation 1 below.

$$\dot{\Omega} = -\frac{3nJ_2R_{\oplus}^2}{2a^2(1-e^2)^2}\cos(i) \qquad (1)$$

where

- J_2 = 0.001082
- R = 6378.135 (km)
- n = mean motion (revs/day)
- a = semi-major axis (km)
- e = eccentricity
- i = inclination (deg)

Nodal precession will cause the debris to spread out and impact a large number of orbits. This creates an interesting condition in that while the overall spatial density of objects in orbit has increased, the likelihood of striking any individual piece of debris from the breakup has decreased. Simply put, the chances of hitting anything in orbit increase, while the chances of hitting anything from that breakup decrease. The image below shows how the FY-1C ASAT debris spreads over time. Of note are the left and right images that show the localized belt of debris and the spread belt of debris respectively.

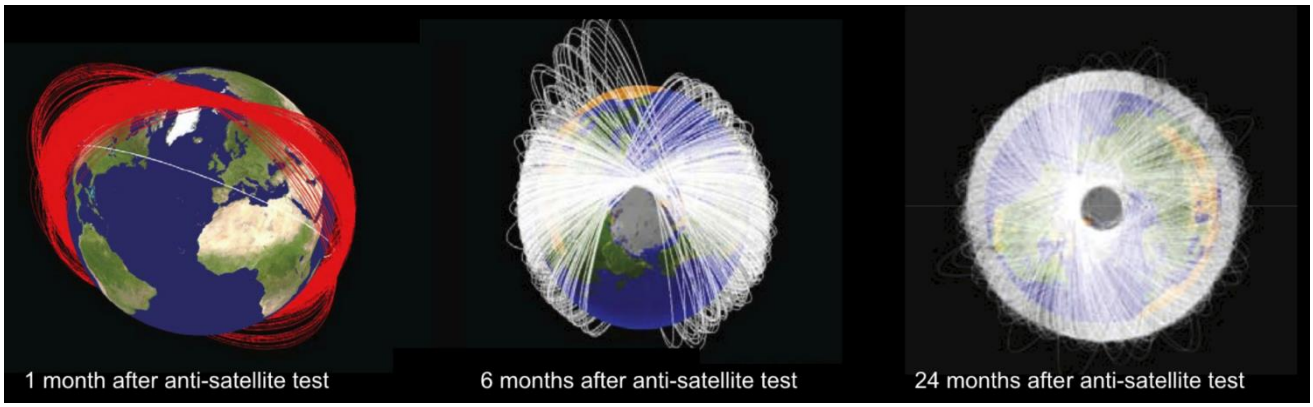

Figure 2. Debris propagation of the FY-1C antisatellite test.

2 APPROACH

Historical data shows the cause of failure for breakups usually involves a propulsion system of some sort [8], but the cause in this simulation was left undefined. Different failures would likely cause different initial spreading of the debris, which could be added in subsequent simulations if desired. The assumed breakup parent object was assigned the orbit characteristics in Table 2.

Table 2. Parent orbit characteristics

Characteristic	Value
Eccentricity	0
Altitude	850 kilometers
Inclination	83°
RAAN	0°
Mean Anomaly	0°
Argument of Periapsis	0°

The zero values were chosen for simplicity of analysis, while the altitude and inclination were chosen for the high spatial density at their location [9]. The thought behind this was to place the breakup in a worst-case location. The scenario begins with the breakup occurring and the pieces are then propagated for one week or until they drop below 120 kilometers, whichever comes first. If a piece meets the minimum altitude condition it is removed from the analysis at that point. The breakup is simulated using STK's Astrogator module to impart an impulsive maneuver on each piece at the same time. The delta velocities are pulled from the NASA EVOLVE model and the direction of the velocity vector is defined in spherical coordinates with azimuth and elevation being pulled from a normal distribution centered at 0° with a standard deviation of 30°. 100,000 pieces of debris distributed uniformly from 3 mm to 1 m were used in this analysis, as listed in Table 3.

Table 3. Breakup event characteristics

Characteristic	Value
Breakup Model	NASA EVOLVE 4.0
# of Pieces	100,000
Piece Material	Aluminum
Min Diameter	3 millimeters
Max Diameter	1 meter
Coefficient of Drag	2.2*
Solar Radiation Pressure (Spherical)	1*
Radiation Pressure (Albedo/Thermal)	1*
Propagator	STK HPOP*

* denotes STK standard value

The minimum diameter was chosen as a piece of this size carries roughly the same energy as a bullet. Pieces below this size are still dangerous but were determined to be out of scope for this effort.

2.1 Simulation Architecture

The simulation begins with user input into a custom Python script. The top of the script contains all the standard modifications that can be made to the simulation. These modifications range from parent orbit parameter and number of debris pieces to the start/end date of the scenario and the normal distribution parameters for azimuth and elevation. This file can be modified on the supercomputer by using the *vi* command to enter and edit the file or on a standard desktop by opening the Python file.

The utility of the supercomputer was critical to the success of this research. For a 100,000-piece desktop scenario, the computation power required would take months to process the job. On the HPC however, this 100,000-piece job was parallelized into 500 instances of the script with 200 pieces in each instance. This reduced the time required from days down to just 105 minutes. The scenario was set up to produce several different kinds of reports. The first set of reports are the characteristics of the debris pieces. For this research, the mass, delta velocity, diameter, area, and area-to-mass ratio was recorded for each piece of debris. Additionally, the scenario produces close approach reports detailing every approach between the debris and catalog within 3 kilometers, as well as a classical orbit element report for each of the pieces in the scenario. Finally, a probability of collision report is generated for each close approach detailing the likelihood of collision as defined by the four different collision models chosen for the research. All the individual debris characteristic files were then concatenated to form 5 files containing 100,000 items each. The close approach and collision likelihood were also concatenated in a similar manner. Finally, with all files concatenated, the data was presented graphically using a mix of pie charts, bar charts, and Gabbard plots. The process is visualized in the activity diagram in Figure 3.

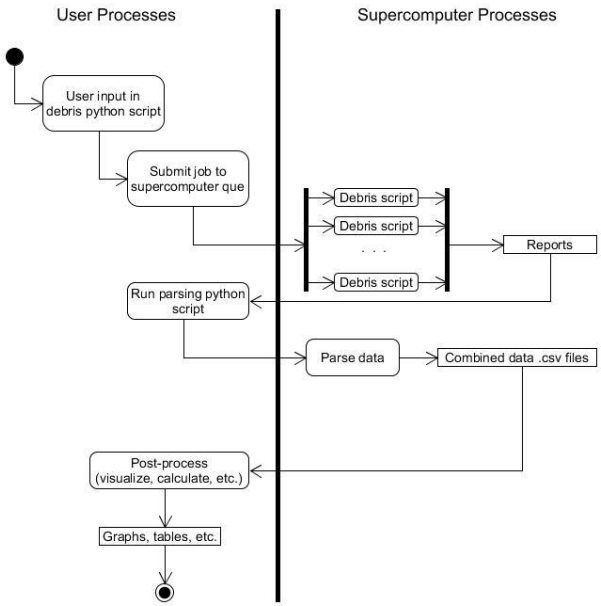

Figure 3. Activity diagram for simulation schema.

2.2 Analysis Strategy

The relative hazard of the debris field was measured by running a close approach analysis using STK's Advanced Close Approach Tool (ACAT). This tool calculates the probability of collision between user-defined primary and secondary objects. The primary objects for this study are the debris pieces, while the secondary object list was comprised of the public catalog of on-orbit objects in the form of the STKAll.tle file. The probability of collision was calculated using four different collision likelihood models: Alfano, Patera, Chan, and Alfano Maximum Likelihood. The four models were chosen to enable a comparison between them and allow for some discussion on the differences in results. A static 1-kilometer threat sphere was set around both the debris and the catalog objects. This was chosen as this is the known collision warning threshold set by the JSpOC [10]. A close approach notification was generated whenever the range between the debris and any objects dropped below 3 kilometers, the setup is best visualized in Figure 4 below. The red line indicates the range measure and the blue line indicates separation

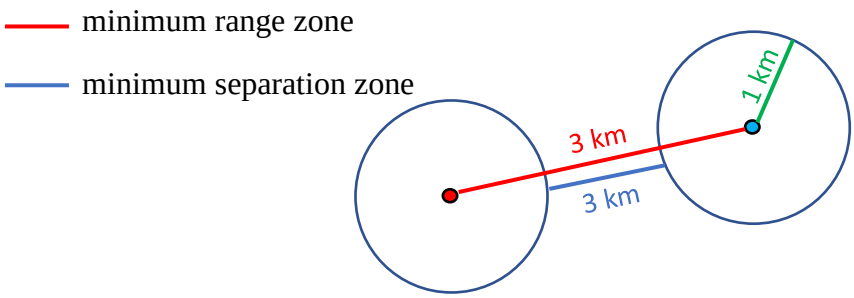

Figure 4. Visualization of generation of close approach notification.

The debris field was analyzed using Gabbard plots. Gabbard plots were developed by John Gabbard during his time at NASA and are used to examine breakup characteristics. The x-axis of the Gabbard plot is the orbital period, while the y-axis is the altitude. This allows for a visualization of the general orbit of the debris pieces and an understanding of the relative impact of the field. It also gives an indication of the lifetime of the pieces by showing which pieces are in lower altitudes and faster periods. In addition to standard Gabbard plots, a modified Gabbard plot was utilized. This plot is similar in that the y-axis remains the altitude, however the x-axis is now the inclination. This plot aids in realizing the spread of the pieces to different inclinations from the parent inclination.

2.3 Results

The results are divided into three sections. The first addresses the characteristics of the debris field as a whole. Secondly, the individual debris piece features are addressed. Finally, the results of the close approach analysis are presented.

2.3.1 Debris Field Characterization

As stated previously, the field was analyzed with both Gabbard and modified Gabbard Plots. Gabbard samples on the first and last day of the analysis week. This was done to see if there was a discernable difference over the course of the week. First, Figure 6 is the FY-1C Gabbard plot that our results will be compared against [11]. Figure 5 is the day one and day seven Gabbard plot of the simulated breakup. Periods greater than 140 minutes were removed to keep the scale on the same order as the FY-1C plot.

The first sample was taken two hours after the initial breakup. The first thing to note is the spread of the debris over the course of one week. This is clearly seen on the left side of the day seven plot. Visually comparing the results of the day seven plot with those of the Chinese ASAT test reveals that the goal of modeling an on-orbit breakup matches what we expect from historical data. By looking at this graph, we can also draw the conclusion that the Chinese ASAT was likely of higher energy than the simulated breakup. This can be seen by the larger angle in Figure 5. The inclined slope of the apogee line shows that there are pieces in more elliptical orbits with higher orbits.

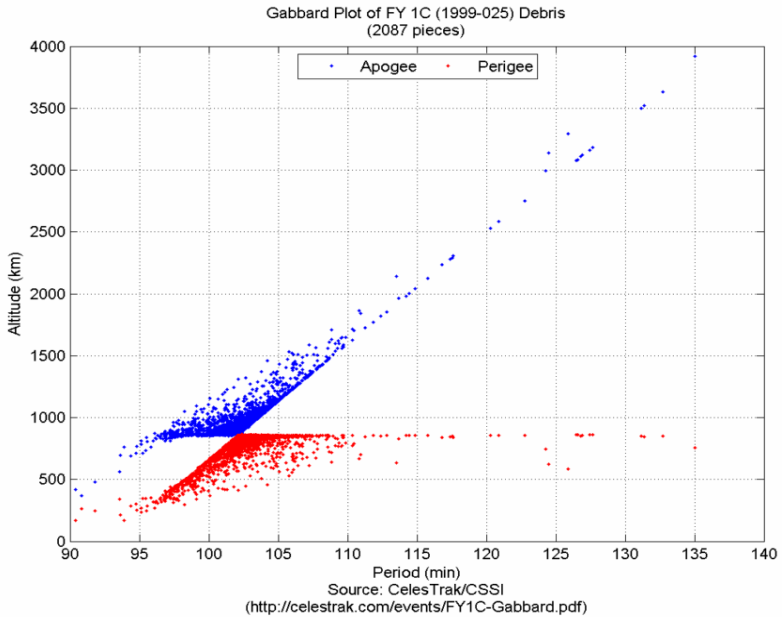

Figure 5. Gabbard plot of FY-1C ASAT test.

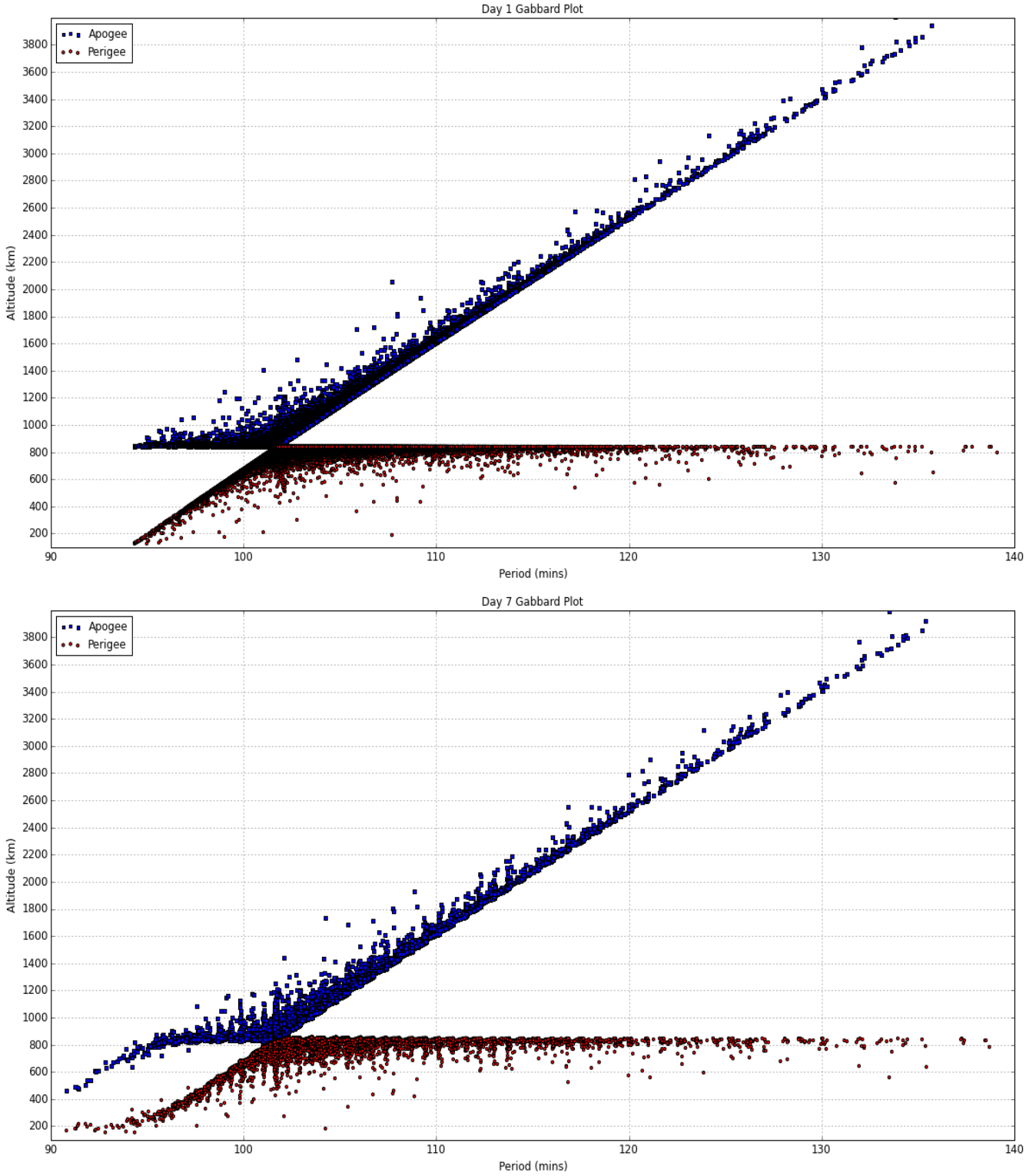

Figure 6. Day 1 and Day 7 Gabbard plots for LEO debris objects.

Modified Gabbard Plots

Next, the modified Gabbard plots for the breakup are presented. As stated previously, these plots are just like standard Gabbard plots, but the y-axis is now inclination. Samples were taken day one and day seven, but only day seven is presented. This is because the average inclination of the field changes slightly (0.0121°) over the course of the week. Figure 7 shows that the average inclination, μ, of the debris field stays around that of the parent object. Additionally, almost all the debris occupies a ± 1.5° (3σ) inclination band around the parent inclination. This information is extremely useful to operators in the absence of actual observations. The bigger concern with debris fields over time is the nodal precession of the pieces, however this nodal change is so small over the course of one week that just knowing the approximate altitude and inclinations effected is the critical information needed for decision makers.

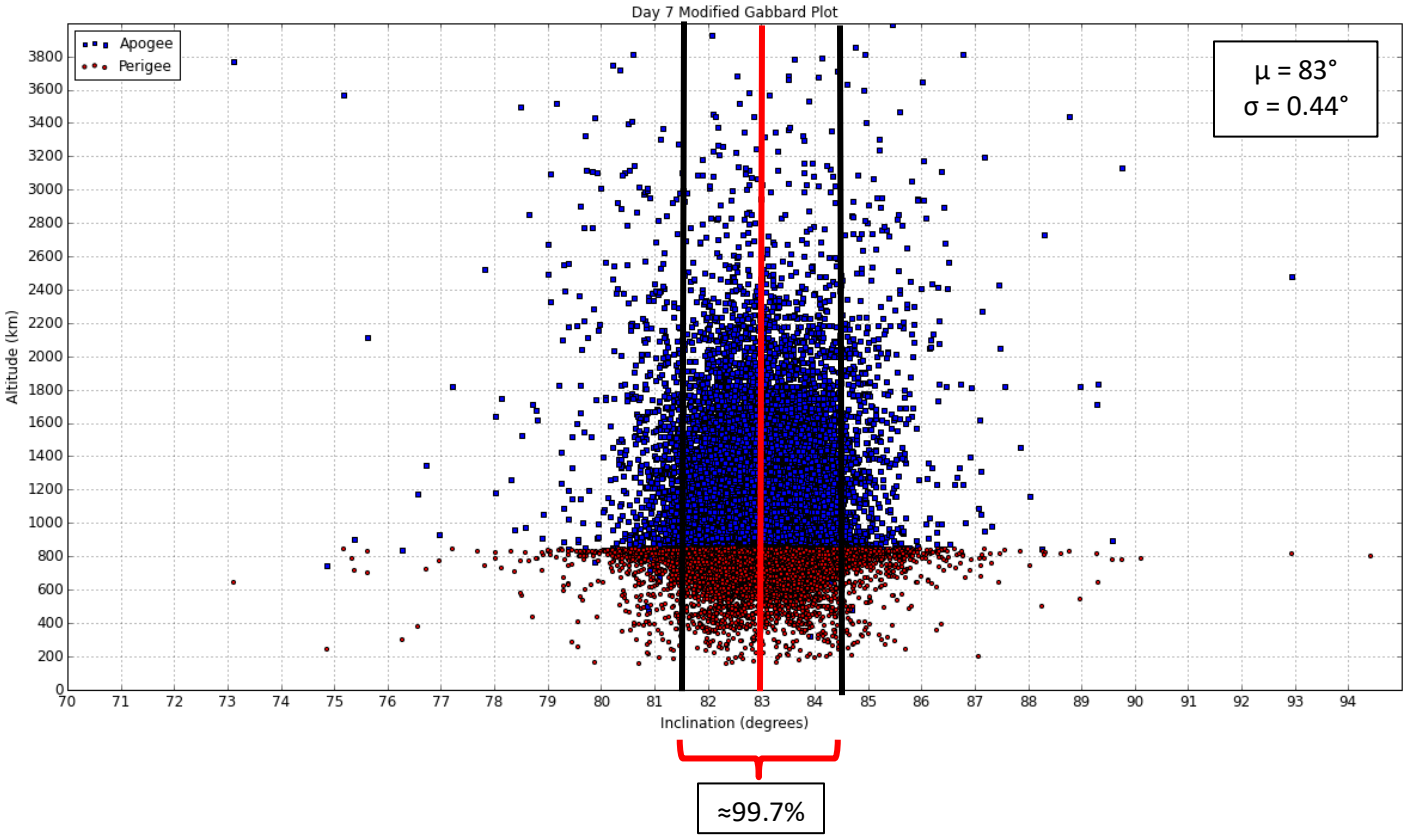

Figure 7. Modified Gabbard plot of debris below 4000 km

2.3.2 Debris Features

Next, in addition to the debris field, it is important to gather data on the individual pieces. First, Table 4 below lists the statistics for the various parameters involved with each debris piece.

Table 4. Debris piece parameter results

Characteristic	Units	Average	Standard Deviation
Area	m^2	0.19	0.17
Mass	kg	3.28	4.06
Area-to-Mass	m^2/kg	0.12	0.21
Diameter	m	0.50	0.29
Δv	m/s	65.35	76.69

All characteristics were generated within the NASA EVOLVE 4.0 model except for diameter, where the minimum and maximum diameter were user specified. The code then created a list of diameters from minimum to maximum with one millimeter spacing. A diameter was randomly pulled from this generated list and plugged into the EVOLVE model. For this case, there were 997 possible diameter choices between three millimeters and one meter.

Nodal Precession

The newly-formed debris will experience the effects of Earth's oblateness. This oblateness will cause the right ascension of the ascending node (RAAN) to precess at a rate defined by Equation 1. The average nodal precession of the debris field was calculated to be -0.76538 deg/day. Table 5 shows how the mean node of the field moves with time. Close attention should be paid to the growth of the standard deviation, as this parameter shows how the belt of debris forms over time.

Table 5. Nodal precession over time

	1 Month	6 Months	1 Year	2 Years
Mean Node (degrees)	332.4	217.6	76.3	203.9
Standard Deviation of Node (degrees)	2.8	11.0	21.0	40.6

From these values, in two years the bulk of the debris will cover a nodal range of ± 120° (3σ). This growth is shown historically by the FY-1C field in FIGURE 8 below.

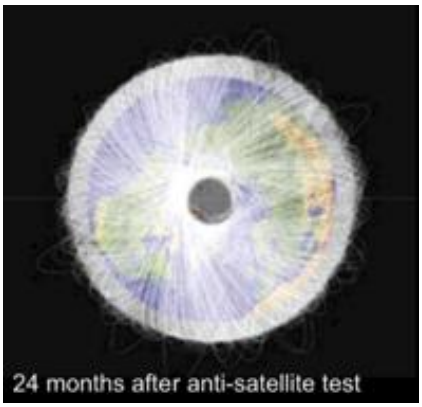

Figure 8. FY-1C debris field spread after two years.

2.3.3 Close Approach Tool Results

As stated above, the close approach tool was configured to report minimum range, minimum separation, and probability of collision for conjunctions with minimum ranges ≤ 3 kilometers. Over the course of one week, there were 725,165 close approaches recorded between the catalog and the debris.

Minimum Range Results

For ease of presentation, the minimum range results were visualized and placed into three different bins. Any conjunction with a minimum range of less than one kilometer was recorded as a "red" encounter. Additionally, anything between one and two kilometers was a "yellow" encounter and anything greater than two kilometers was deemed a "green" encounter. The weighted average minimum range for all close approaches was 2.0544 kilometers with a standard deviation of 0.0144 kilometers. Of these conjunctions, 79,300 (~11%) were within the one-kilometer red zone and 240,812 (~33%) were within the two-kilometer yellow zone. Furthermore, of the red zone conjunctions, roughly 2.5% were within 500 meters. For reference, SOCRATES, a close approach warning tool system for the Center for Space Standards and Innovation, predicted a closest approach of about 584 meters for the Iridium/Cosmos collision [12]. The results are shown in Figure 9.

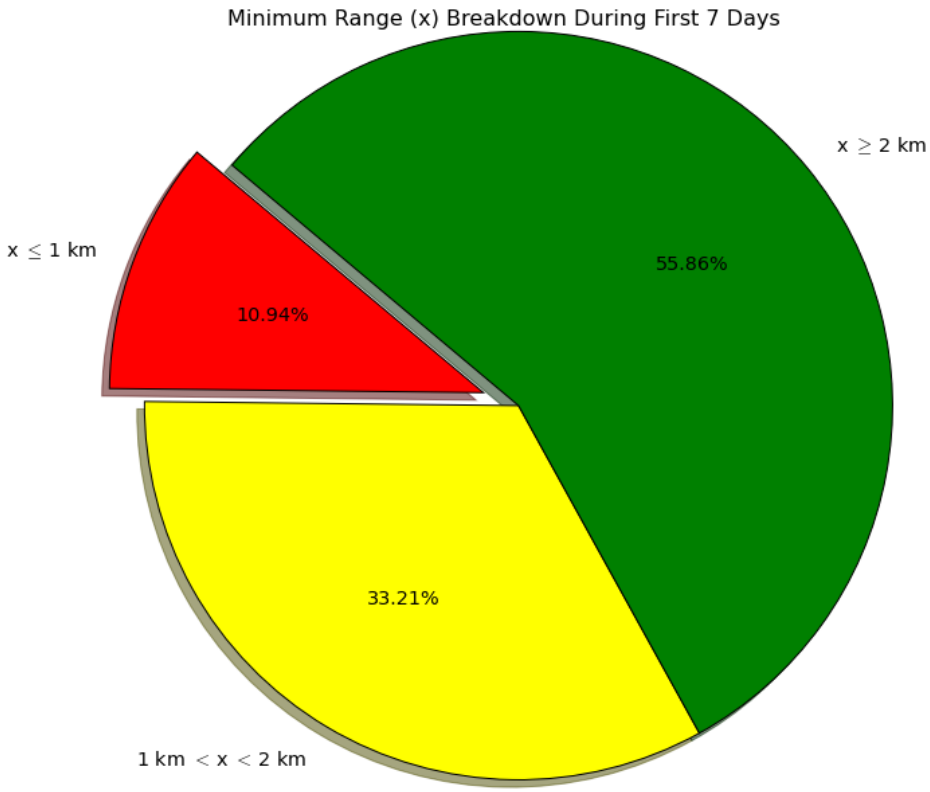

Figure 9. Distribution of minimum range zones within first week after breakup event

Minimum Separation Results

The minimum separation parameter is the distance between the threat spheres of each of the pieces. This parameter ranged from zero kilometers (threat spheres intersect) to one kilometer. A similar binning approach was taken for this data as well. For this data, it made sense to divide it into quarter kilometer increments, so a fourth color was added. Red encounters were less than 250 meters, orange encounters were between 250 and 500 meters, yellow encounters are between 500 and 750 meters, and green encounter were anything greater than 750 meters. The results are shown in Figure 10. The weighted average was found to be 0.5346 kilometers with a standard deviation of 0.01 kilometers.

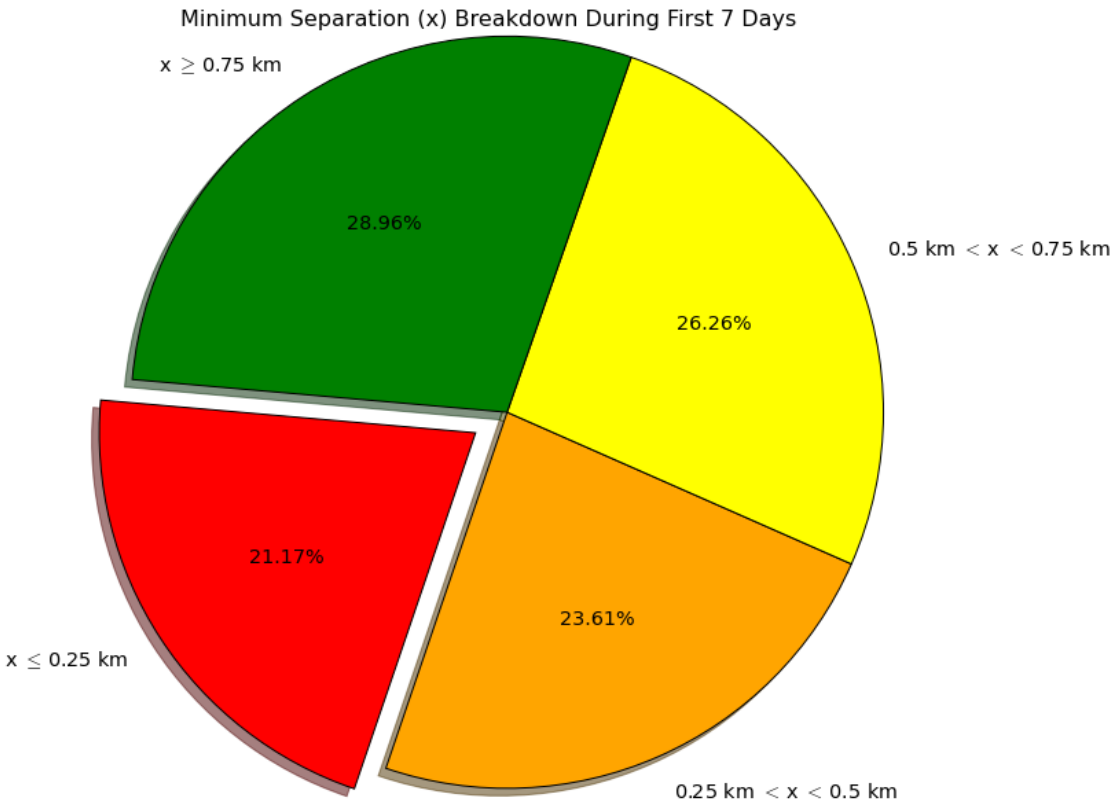

Figure 10. Distribution of minimum separation zones within first week after breakup event

Probability of Collision Results

The probability of collision for all 725,000 close approaches was calculated using four different linear probability models. For each model, the maximum, minimum, mean, and standard deviation was reported. Additionally, the average daily and weekly chance of at least one collision was reported for each model. The average chance of collision calculations were done assuming that each event was independent. This leads to the use of the inclusion-exclusion principle as defined by Equation 2 below.

$$\mathbb{P}\left(\bigcup_{i=1}^{n} A_i\right) = \sum_{i=1}^{n} \mathbb{P}(A_i) - \sum_{i<j} \mathbb{P}(A_i \cap A_j) \quad + \sum_{i<j<k} \mathbb{P}(A_i \cap A_j \cap A_k) - \cdots + (-1)^{n-1}\, \mathbb{P}\left(\bigcap_{i=1}^{n} A_i\right) \qquad (2)$$

The data for this research was unique in that the individual likelihood of collision was so low (on the order of 10E-07) that it causes the values in Equation 2 to come out on the order of

$$\mathbb{P}\left(\bigcup_{i=1}^{n} A_i\right) = \sum_{i=1}^{n} \mathbb{P}(A_i) - \sum_{i<j} \mathbb{P}(A_i \cap A_j) \quad + \sum_{i<j<k} \mathbb{P}(A_i \cap A_j \cap A_k) - \cdots + (-1)^{n-1}\, \mathbb{P}\left(\bigcap_{i=1}^{n} A_i\right) \qquad (3)$$

10E-02 10E-07 10E-15

This means that the daily chance of collision is essentially dominated by the first term, leading to an approximation of the daily chance of collision being defined by

$$\mathbb{P}\left(\bigcup_{i=1}^{n} A_i\right) \approx \sum_{i=1}^{n} \mathbb{P}(A_i) \qquad (4)$$

Furthermore, once the values were calculated for each day of the week, they can be rolled up into the weekly chance of at least one collision using Equation 2. Since the values were on the order of 10E-02 at this point, the full inclusion-exclusion principle was used. The results for each probability model are shown Table 6.

Table 6. Linear probability model results

	Chan	Alfano	Patera	Max
μ (weighted)	3.96E-07	3.96E-07	3.96E-07	2.16E-06
σ (weighted)	4.94E-09	4.94E-09	4.94E-09	4.06E-07
Maximum	1.00E-06	1.00E-06	1.00E-06	5.35E-02
Minimum	1.05E-07	1.05E-07	1.05E-07	1.64E-07
Chance of at Least 1 Collision (Average Daily)	4.100%	4.100%	4.100%	22.332%
Chance of at Least 1 Collision (Average Weekly)	25.699%	25.548%	25.389%	62.817%

The first three models are very similar in their evaluations of the collision likelihood. This is because they are all solving the same equation but taking different approaches. Additionally, the last column of data can be viewed as the worst-case scenario. This assumes the worst possible collision geometry and predicts the maximum likelihood of collision. At first, this data appears to be frightening, but this assumes that every one of the 700,000 conjunctions have the worst possible geometry. This type of analysis is better suited for individual close approaches where an analysis of all outcomes is needed to determine a course of action. Ultimately, what can be gained from this analysis is that a simple choice of the first three models is sufficient for close approach analysis.

3 CONCLUSION AND FUTURE WORK

The primary goal of this research was to leverage an HPC to model a large-scale on-orbit breakup. This was accomplished and reduced to the real time to run the scenario to under two hours. The next step beyond modeling the field was to understand the dangers that such a field would impose on the space environment. The ACAT from STK opened the door to running a close approach analysis with the debris pieces and current on-orbit catalog. This allowed for quantification of risk to be performed by demonstrating the number of close approaches and probability of collision over the course of one week. Finally, the last objective was to constrain the timeline to produce meaningful results in a reasonable amount of time. Analyzing the impact to the space environment over the course of week means nothing if it takes longer than a week to get results. The goal was to produce results within an average LEO orbit (90 minutes) or less. The current schema produced results in 105 minutes. While this did not meet the stated objective, further parallelization or code optimization could likely get the results to well within the desired notification timeline.

The original plan for this research was to not only generate and analyze a debris field, but also to produce a reaction plan to such an event. The reaction plan has not yet been produced. The next step would be to take the results of the simulation and then optimize maneuvers to reduce impact to fuel and mission effectiveness. Essentially, it would be a minimization of probability of collision subject to a few constraints. The primary constraint proposed is fuel consumption as this is a direct indication of impact to mission life. Constraints on maximum altitude or inclination change could also be included. This would act as the mission effectiveness constraint by keeping the spacecraft contained to an "operational regime." This would ultimately lead to operational plans to respond to an on-orbit breakup given some basic initial knowledge about the breakup.

Additionally, this work could be revisited to further optimize the current schema and reduce the computational burden and therefore the time to report results. Further model improvements would be to use more realistic debris distributions observed from other debris-producing events rather than a uniform distribution on diameter.

ACKNOWLEDGEMENTS

The authors would like to acknowledge AGI for granting access to not only their STK software but also their ACAT module for use on the high-performance computer.

REFERENCES

[1] United Nations Office for Outer Space Affairs, "Space Debris Mitigation Guidelines of the Committee on the Peaceful Uses of Outer Space," *United Nations Publ.*, p. 12, 2010.

[2] M. Wall, "Space.com Envisat Article May 2012," *Space*, 2012. [Online]. Available: http://www.space.com/15640-envisat-satellite-space-junk-150years.html. [Accessed: 29-May-2017].

[3] European Space Agency, "Copernicus Sentinel-1A Satellite Hit By Space Particle," *ESA*, 2016. [Online]. Available: http://www.altestore.com/store/Solar-Panels/51-to-99-Watt-Solar-Panels/BP-Solar-585U-85W-12V-Solar-Panel/p2708/. [Accessed: 08-Aug-2017].

[4] T. S. Kelso, "Analysis of the 2007 Chinese ASAT Test and the Impact of its Debris on the Space Environment," *Adv. Maui Opt. Sp. Surveill. Technol.*, pp. 321–330, 2007.

[5] T. S. Kelso, "SATCAT Growth," *CelesTrak*, 2017. [Online]. Available: http://www.celestrak.com/satcat/growth.png. [Accessed: 10-Aug-2017].

[6] R. Thompson, "Aero Corp Space Debris Primer," *Crosslink*, Dec-2015. [Online]. Available: http://www.aerospace.org/crosslinkmag/fall-2015/a-space-debris-primer/.

[7] NASA, "Orbital Debris Quarterly News July 2010," *Orbital Debris Q. News*, vol. 14, no. 3, pp. 1–12, 2010.

[8] N. L. Johnson, E. Stansbery, D. O. Whitlock, K. J. Abercromby, and D. Shoots, "History of on-orbit satellite fragmentations 14th edition," *Houst. NASA*, no. June, 2008.

[9] National Research Council, *Orbital Debris A Technical Assesment*. Washington, DC: National Academy Press, 1995.

[10] J. W. Wagner, "Beware the situation: how JSpOC tracks space debris," *Room Sp. J.*, vol. 1, no. 1, 2014.

[11] T. S. Kelso, "CelesTrak: Chinese ASAT Test," *CelesTrak*, 2012. [Online]. Available: https://celestrak.com/events/asat.asp.

[12] T. S. Kelso, "CelesTrak Iridium Cosmos," *CelesTrak*, 2012. [Online]. Available: http://celestrak.com/events/collision/. [Accessed: 29-May-2017].